Journal of Peptide Science
J. Peptide Sci. **11**: 463–471 (2005)
Published online 10 January 2005 in Wiley InterScience (www.interscience.wiley.com). DOI: 10.1002/psc.636

JOURNAL OF PEPTIDE SCIENCE

Peptide dynamic fingerprints: a tool for investigating the role of conformational flexibility for GLP-1 analogs affinity

M. ADENOT,[a*‡] C. SARRAUSTE DE MENTHIÈRE,[c‡] A. KERVRAN[b] and G. GRASSY[a]

[a] Centre de Biochimie Structurale, 15 avenue Charles Flahault, 34060 Montpellier Cedex, France
[b] INSERM U-376, CHU Arnaud de Villeneuve, 34295 Montpellier Cedex 5, France
[c] Institut de Génétique Humaine, CNRS UPR1142, 141 rue de la Cardonille, 34396 Montpellier Cedex 5, France

Received 29 July 2004; Accepted 23 September 2004

Abstract: Glucagon-like peptide-1 (GLP-1) is a 30-residue peptide implicated in short-term appetite regulation. Its analogs are presumed to be potential drugs against obesity and non-insulin dependent diabetes mellitus (NIDDM or type 2 diabetes). This study examined how the dynamic fingerprints can be used for establishing dynamics–activity relationships in a series of peptides for which the mechanism of action is unknown and in which mutations can cause an increase or decrease in biological activity. The 3D autocorrelation method was used to generate maps of both active and inactive analogs. As the active conformation of GLP-1 is not yet clearly defined, the dynamic fingerprints of peptides in an aqueous environment were compared to explain the high affinity of the peptide for its receptor. The suggestion that the peptide could bind to the receptor in a folded conformation has been examined. In the case of the GLP-1 analogs, it was shown that the folding tendency cannot be directly related to affinity values and the results do not favor a folded active conformation model of GLP-1.

Keywords: molecular dynamics; glucagon-like peptide; conformational autocorrelation method; dynamics–activity relationships

INTRODUCTION

Glucagon-like peptide-1 is a 30-residue peptide released from L-cells in the small intestine as well as from pancreatic alpha-cells in mammals. The truncated form GLP-1(7–36)amide exhibits an insulinotropic action and a lowering effect on glucagon secretion resulting in a very interesting antidiabetogenic effect. The glucose-reducing effect is self-limiting as it depends directly on the level of glycemia; it will protect against hypoglycemic reaction, which is the most acute side-effect of the current sulfonylurea antidiabetic therapy. Unlike leptin, GLP-1 is implicated in the short-term regulation of appetite. For these reasons, GLP-1 has been considered a very important drug candidate in the treatment of non-insulin-dependent diabetes mellitus and obesity. Furthermore, GLP-1 inhibits gastric secretion, delays gastric evacuation and is implicated in inter-meal satiety signalling. Overfeeding causes an increase of post-prandial GLP-1 release and elicits a normal satiety signal. Obese subjects seem to have an attenuated GLP-1 release in response to meals. Intracerebral injections of GLP-1 in rats will inhibit food intake but the question has not yet been answered as to whether long-term administration of GLP-1 will influence appetite in man.

GLP-1 receptors have been found in the lung, the stomach, the brain and the pancreas where their stimulation inhibits glucagon release in alpha-cells and stimulates insulin release in beta-cells. The GLP-1 receptors are very specific: in spite of a high sequence homology in the glucagon/GLP family, none of these peptides show a better activity at the receptor than GLP-1 itself [1] and exendin-4, a 39-amino acid peptide extracted from *Helodermantidae* venom. Using international notation, the actual GLP-1 sequence is H^{7}AEGTFTSDVSSYLEGQAAKEFIAWLVKGRG^{37}-NH2. Here, the convention is employed whereby the first amino acid in GLP-1 (His) is designated number 1. The native molecule studied here is GLP-1-(7–37) derived by truncation of the larger molecule GLP-1-(1–37).

Structure–activity relationships have been investigated to highlight the importance of the HAE *N*-terminal tripeptide for binding and the *C*-terminal region in the activation of the receptors [2,3]. Ala-scan studies have been undertaken to identify the specific amino acids that are important for receptor-binding and activation but the published results are not in agreement [4,5].

From a structural point of view, in aqueous solution, the GLP-1(7–36)amide is recognized as largely random coils by Thornton [6] but GLP-1(7–36) shows 50% beta-sheet content in circular dichroïsm [7]. The structure of GLP-1(7–36)amide determined by Thornton in a membrane-like environment of dodecylphosphocholine micelles is largely helical and similar to that observed for glucagon [8]: two amphiphilic segments (7–14) and (18–29) and a linker region (15–17). The structural

Abbreviations: DPP IV, dipeptidyl-peptidase IV; GLP, glucagon-like peptide; MD, molecular dynamics; MLP, molecular lipophilic potential.

* Correspondence to: Dr M. Adenot, Synt:em, Parc Scientifique G. Besse, 30000 Nimes, France; e-mail: madenot@syntem.com
‡ These authors contributed equally to this work.

requirements as well as the bioactive conformation of the peptide binding to its receptor are not well established even if it has been suggested that a fold or turn of the peptide backbone may cause close steric vicinity of the *N*-terminus and *C*-terminus of GLP-1-(7–36)-NH_2 in solution [5,9]. It is possible that this structure is stabilized by the formation of an ionic bond between the side-chains of Arg^{30} and Glu^3 (or Asp^9). From Ala-scan studies [4,5] it has been shown previously that the replacement of Arg^{30} with an alanine induced a significant decrease in both affinity and activity ($IC_{50} = 4.6 \pm 0.6$ nM and $EC_{50} = 7 \pm 5$ nM for [A^{30}]GLP-1-(7–36)-NH_2 versus 0.25 ± 0.09 nM and 2.6 ± 0.4 nM for GLP-1-(7–36)-NH_2 itself) [4]. In contrast, the deletion of Arg^{30} improves the potency since [desR^{30}]GLP-1-(7–37)-NH_2 is more active than GLP-1-(7–37)-NH_2 [9]. It appears that this result is not general: for some derivatives ([F^1], [L^2], [V^2], [e^3], [S^3] and [K^3]GLP-1-(7–37)-NH_2), the deletion of arginine reduces more or less both the binding and the production of cAMP. For other ([D^3], [L^3] and [M^3]GLP-1-(7–37)-NH_2) this deletion produces powerful agonists. For example, [D^3-desR^{30}]GLP-1-(7–37)-NH_2 is slightly more active than exendin-4, the most powerful GLP-1 agonist known today – which does not present arginine at position 30 [10].

The fact that suppression of the only arginine present in the GLP-1 sequence gives rise to derivatives at least as potent as the native hormone, is a strong indication that, if a turn or fold was required for full biological activity, Arg^{30} was not implicated in its stabilization.

The characteristic helix-linker-helix structure of GLP-1 and the fact that both *N*- and *C*-extremities have been implicated in the activity of the peptide could suggest an important flexibility in the central part of the peptide. When positions 9–25 were replaced by a GEWTYDDATKTFTVTE sequence hairpin to help the extremities draw closer and to facilitate the peptide folding to a more compact conformation, no higher activity or affinity level for this analog (data not shown) were obtained. However, this observation cannot actually exclude that GLP-1 interacts in a folded conformation; the local modification of the central part of the peptide could explain a loss of activity, whatever the conformation adopted by the peptide. Knowledge of which of the folded or unfolded conformations is interacting with the receptor is a crucial question for the design of peptidic or pseudo-peptidic analogs of GLP-1. Searching for bioactive conformations of flexible molecules such as peptides in the absence of any template structure is a hazardous task. Based on the idea that all active candidates could share a common folded conformation or a set of local internal constraints, which can be further examined for local pharmacophoric features, systematic molecular dynamics trajectories comparisons were performed. In a previous paper [20], the conformational autocorrelation method was used successfully to design immunosuppressive compounds. Here, this methodology was applied to use an early dynamic feature of GLP-1 as a fingerprint and to study the consequences of conformational change on the amphiphilic character of the peptide. The impact of mutations at positions 1 and 2 of GLP-1 have been analysed in molecular dynamics trajectories by use of the conformational autocorrelation method [11].

METHODOLOGY

Peptide Synthesis and Purification

The following peptides were synthesized and tested *in vitro*: [Y^1]-GLP, [W^1]-GLP, [F^1]-GLP, [S^2]-GLP, [L^2]-GLP, [V^2]-GLP and [a^2]-GLP (the letter 'a' refers to D-alanine).

Reagents. Tyr^1-cAMP, IBMX, bacitracin and BSA (fraction V) were purchased from Sigma Chemical Co (St Quentin Fallavier, France). Na[^{125}I] (2.000 Ci/mmol) was obtained from DuPont NEN (Mechelen, Belgium). Mono-[^{125}I]-labeled GLP-1-(7–37)-NH_2 and mono-[^{125}I]Tyr1-cAMP were obtained by the chloramine-T procedure and purified by reverse-phase HPLC on μBondapak C18 column (Waters, Milford, MA, USA). All the compounds used for solid-phase peptide synthesis (resins, coupling reagents and protected amino acids) were from PerSeptive Biosystems (Framingham, MA, USA).

Peptide synthesis. Peptide synthesis was carried out on a 0.15 mmol scale using a continuous flow apparatus (PerSeptive Biosystems, model 9050 PepSynthesizer) starting from Fmoc-PAL-PEG-PS-resins. All N-α-Fmoc amino acids in 4-fold excess were assembled using diisopropylcarbodiimide and 1-hydroxybenzotriazole as coupling reagents. Peptides were cleaved from the resin and deprotected using K reagent. Each crude peptide was purified by semi-preparative HPLC on a Δpack column (20×250 mm, Waters) using various acetonitrile gradients in aqueous 0.1% TFA. The purity of the collected fractions was established by analytical HPLC on Lichrosphere-100 RP-18 columns (Merck, Darmstadt, Germany) and by electrospray ionization mass spectrometry (VG Trio 2000, Fison Instruments, Manchester, UK). For all the peptides synthesized, amino acid analyses and mass spectra were in complete agreement with the proposed structures.

Affinity Binding Tests

Cell cultures and membrane preparations. RIN T3 cells (obtained from Dr L. Pradayrol, INSERM U151, Toulouse, France) were grown in DMEM containing 5.5 mM glucose (Life Technologies, Eragny, France), and supplemented with 10% fetal calf serum, 100 IU/ml penicillin and 100 µg/ml streptomycin [12]. Plasma membranes from RIN T3 cells were prepared according to a previously described method [12] and stored at −80 °C until used. Membrane proteins were measured using the Bradford assay with BSA as standard [13].

Binding studies. Binding experiments with RIN T3 membranes were performed in 60 mM Tris-HCl buffer (pH 7.5) containing 4% BSA and 750 µg/ml bacitracin. Membranes (20–30 µg)

were incubated in a final volume of 500 µl with ~15 fmol of ^{125}I-GLP-1-(7–37)-NH_2 (50 000 cpm) and unlabeled competitor ligand or analogs for 45 min at 37 °C, as described previously [12]. The reaction was stopped by addition of 750 µl ice-cold KRB (pH 7.5) containing 3% BSA, centrifuged at 4 °C for 5 min at 12 000 × **g**. The pellet was rinsed with 1 ml of ice-cold KRP, sedimented by another centrifugation step, and counted for radioactivity. Nonspecific binding was determined in the presence of 1 µM GLP-1-(7–37)-NH_2 and was subtracted from each value. Binding data were analysed using a version of the Ligand program (release 2.0, Biosoft). IC_{50} values were deduced by fitting the experimental data according to the Hill equation.

Cyclic AMP production. RIN T3 cells were grown in 24-well plates for 6 days and the medium was changed 1 day before experiments. Cells (0.30 ± 0.03 10^6 cells/well; $n = 10$) were washed twice with DMEM before the addition of 0.5 ml DMEM supplemented with 1% BSA and 0.2 mM IBMX and containing the test peptides. After a 20 min incubation at 25 °C, cellular cAMP was extracted, succinylated and quantified by radioimmunoassay [14–16]. The data are presented as a percent of maximal stimulation. 100% cAMP production corresponds to the maximal production above basal (5–8 fold) obtained by 10^{-8} M GLP-1-(7–37)-NH_2 and 0% cAMP production corresponds to the basal production in the absence of GLP-1-(7–37)-NH_2 or analogs. The EC_{50} values were calculated from the Hill equation.

Molecular Dynamics Simulations

The starting structure for the minimization and MD calculations was the Thornton conformation. Peptide models were obtained from the Thornton model by a simple mutation of side chains [6]. The monitoring of root mean square fluctuations during a preliminary 2000 ps simulation showed that the folding occured at about 600 ps and an equilibrium was reached after folding at about 1000 ps for GLP-1. While peptide folding could be a critical step to select peptides with higher affinity, trajectories were truncated at 1000 ps. All structures were immersed in a 2269 molecules rectilinear water box (65 Å × 35 Å × 30 Å). Molecular mechanics calculations were performed using the all-atom force field as implemented in the AMBER 7.0 software (University of California San Francisco). All parameters were default. Energy minimization and molecular dynamics simulation were carried out on a Silicon Graphics Indy workstation. The system was energy minimized according to the following preparatory equilibration procedure: (i) 10 ps of molecular dynamic of the solvent only with progressive heating (homogenization step), (ii) 500 steps of solvent minimization (steepest descent relayed by conjugate gradient) and (iii) a minimization of the total system (solute + solvent) with a progressive removal of the constraints from the solute (100, 50, 30, 10 and 0 kcal/mol). During the molecular dynamics itself, the temperature of the system was first gradually increased from 10 to 300 K. A constant temperature simulation was then performed at 300 K. The total simulation time was 1000 ps, including the 10 ps heating step time.

Single trajectories have been released for GLP-1 itself and seven analogs varied at position 1 or 2. In the absence of multiple initial conditions and any reference conformation to which comparisons can be made, a single trajectory for a peptide does not necessarily represent the ensemble reasonably well. However, the primary intention was not necessarily to seek for realism in trajectory but to apply molecular dynamics as a theoretical filter to detect a set of internal constraints in the central part of the simulated peptide which may be associated with variations of biological activity.

Simultaneous Comparison of Dynamic Trajectories for Different Molecules

The graphical trajectory animation tool provides a convenient, but not accurate, method to evaluate the similarity of dynamic behaviour between two different molecules. The 3D autocorrelation method (3D ACM) has been initially developed to compare molecular trajectories of a protein obtained with different adjustable parameters and contribute to the rational choice of molecular dynamic simulation parameters [11]. Then, it has been successfully applied to the virtual screening of immunosuppressive peptides [18]. The conformations generated during the MD simulations were converted to vectors using the 3D autocorrelation method [19] and then projected into a 3-principal component space using a Principal Components Analysis. All calculations were performed using Tsar software [17]. Trajectories from several analogs of the same size in similar computational conditions can be compared at a glance by projection onto the GLP-1(7–36)amide reference trajectory.

Molecular Lipophilic Potential (MLP) Calculation

The molecular lipophilic potential is largely recognized as an important concept for understanding hydrophobic interactions between surfaces or solvent/solute interfaces [20]. The MLP is defined by the value of the tabulated hydrophobic fragmental constants f_x [21] at each point in a space around the molecule. In order to take the proximity effects into consideration, a distance-dependent function is introduced into the MLP calculation. Graphic representation of the MLP equipotential surfaces uses a color scale to discriminate between hydrophobic and hydrophilic surfaces. As it was of interest to visualize the evolution of the MLP during the dynamic simulation, it was displayed for both folded and unfolded conformations using MOLCAD module from Sybyl 6.9 software (Tripos) on a Silicon Indy workstation.

RESULTS

Affinities and Activities of the GLP-1 Analogs

The biological results for analogs mutated in the *N*-terminal part of the peptide, at positions 1 and 2, are summarized in Table 1. Mutation at position 1 led to both an agonist ([F^1]-GLP) and a weak antagonist ([W^1]-GLP). A calculation of 14 side chain descriptors [36] showed that the molecular volume at position 1 discriminates between active peptides (volume lower than 120 $Å^3$) and inactive peptides (volume greater than 125 $Å^3$). Furthermore, a previous QSAR study [37] showed that the presence of a ring as well as a basic

Table 1 GLP-1 Analogs Included in the Test Set

Peptide	Affinity IC_{50} (nM)	Activity ED_{50} (nM)
GLP-1	0.26 ± 0.01	0.8 ± 0.1
[F^1]-GLP-1	0.38 ± 0.06	1.1 ± 0.4
[Y^1]-GLP-1	2.71 ± 0.28	9.8 ± 3.2
[W^1]-GLP-1	3.3 ± 0.6	127 ± 35
[S^2]-GLP-1	2.9 ± 0.3	15.1 ± 6.3
[a^2]-GLP-1	0.15 ± 0.01	0.8 ± 0.4
[L^2]-GLP-1	5.7 ± 1.7	180 ± 62
[V^2]-GLP-1	0.47 ± 0.04	2.6 ± 0.81

function at position 1 seem to be critical for the GLP-1 action.

In the conformation adopted in membrane-like environments, the *N*-terminal part displays a great conformational lability [6], so that it is possible that the positively charged imidazolyl group of His^1 would be attracted to the negatively charged carboxylic group of Asp^9 as is assumed in glucagon [29–33]. This latter hormone and GLP-1 possess highly homologous *N*-terminal sequences ($H^1SQGTFTSD^9$- and $H^1AEGTFTSD^9$- respectively) in which the first histidine is separated from an aspartic acid by seven residues. Starting with this hypothesis and a model based on the Thornton and Gorenstein results [6], in which the residues 7–14 and 18–30 belong to two separated helices, attention was given to the fact that the side chains of His^1 and Asp^9 become closer in potentially active conformations.

A consideration of interactions occuring in the large planar loop formed in the *N*-terminal region of the GLP-1 molecule in the receptor-bound state allowed the interpretation of these results and observations previously reported in the literature.

In such a case, it appears that the methyl group of Ala^2 is directed towards the inside of the loop, so that mutations at this position, carried out with residues having a long side-chain, such as leucine, destabilize the structure by interacting with the amino acids facing it (Thr^5). Under these circumstances, position 2 can accommodate valine without a dramatic change in activity, but not leucine. In the case of [S^2]GLP-1, electrostatic repulsions occur between the hydroxyl and the carbonyl groups belonging respectively to Ser^2 and His^1, thus destabilizing the *N*-terminal structure. This explains the loss in biological activity observed for the analog having a serine in position 2 in comparison with GLP-1. The change in chirality, L-Ala^2 → D-Ala^2, stabilizes the loop by positioning the methyl group towards the outside of the loop so that the analog [a^2]GLP-1 is at least as active as the native hormone.

The position 2 residue is of considerable interest since Ala^2 is the target residue for the proteolytic enzyme DPP IV [22], a widely distributed and highly specialized aminopeptidase, which removes dipeptides from peptides with a *N*-terminal penultimate proline or alanine. Since an intact *N*-terminal is required for GLP-1 biological activity, hydrolysis by DPP IV present in human serum may play a major role in inactivating the peptide hormone *in vivo* [23–26]. Therefore, in order to design compounds displaying enhanced metabolic stability, it is of primary importance to find active analogs with residues differing from Ala or Pro in position 2.

As previously reported [24,27,28], analogs of GLP-1 with D-Ala or small amino acids (Gly and Aib) in position 2, bind to the receptor with high affinity and are active in isolated pancreas. This study confirms that the stereochemistry at this position is of lower importance, since [a^2]GLP-1 displays the same activity as GLP-1. In contrast, the replacement of Ala^2 by a serine, found at the same position in several peptides of the GRF superfamily, reduced the affinity for the receptor by a factor of 10 and the production of cAMP by about a factor of 20. This decrease in activity might be related to an increase in polarity rather than volume. Indeed, at this position steric bulk seems to have little importance, since [V^2]GLP-1-(7–37)-NH_2 in which Ala^2 was replaced by a valine, which is more voluminous than a serine, retains significant biological activity; its receptor affinity and cAMP production were only reduced by about two- and three-fold, respectively. However, beyond a certain value the side-chain volume is critical since [L^2]GLP-1 displayed a ~20-fold reduction in the receptor affinity, associated with a 200-fold reduction in receptor activation. Like [W^1]GLP-1, [L^2]GLP-1 is a weak antagonist of the GLP-1 receptor.

These results highlight the significance of both steric hindrance and polarity associated with the amino acid side-chain located in position 2.

GLP-1 Molecular Dynamics

During the trajectory, the two extremities of GLP-1 draw closer through a distinct bending of the central part of the peptide, around the amino acid Gln17 (Figure 1). It is noticeable that this characteristic motion is also observed when an extended conformation is used as a starting point. The initial bend angle between the two helical axes is 141°. The folding of GLP-1 begins early and occurs continuously until it reaches its maximum after 725 ps with a bend angle around 70°. Then, after 1000 ps simulation, the bend angle wavers between 90° and 110° (Figure 2). The description of the trajectory by 3D ACVs provides a global view of the simulation through the 3D autocorrelation profile and a graphical representation of the conformational space explored during the dynamics. Principal components analysis of the 3D autocorrelation vectors is graphically represented for

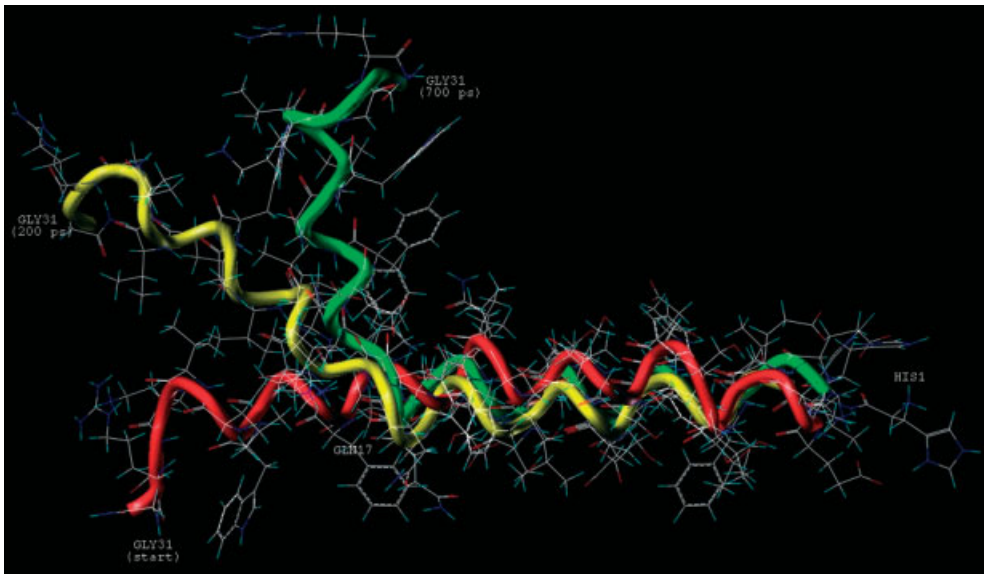

Figure 1 The folding process of GLP-1 during the molecular dynamics trajectory. Conformations are represented at 0 ps (red), 200 ps (yellow) and 700 ps (green). The maximum bend occurs at 725 ps with a bend angle equal to 70°.

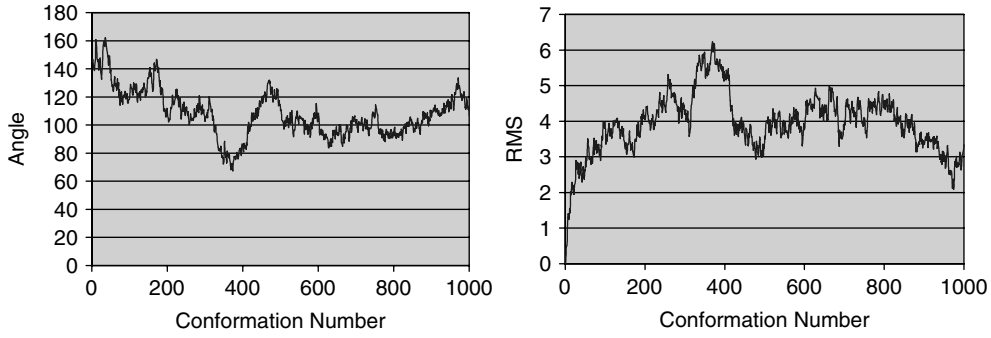

Figure 2 Monitoring of bend angle (Cα[1]-Cα[17]-Cα[31]) and RMS deviation of (7–37)-GLP-1 during a 2000 ps MD trajectory (1 conformation saved every 2 ps).

the first 1000 ps trajectory in the space defined by the first three principal components (>80% of the total variance): the dynamic fingerprint appears as a continuous structure with a soft transition from original to folded conformations (Figure 3). The flexibility

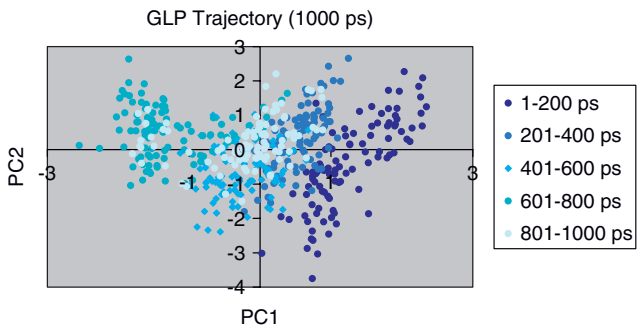

Figure 3 Projection of the (7–37)-GLP-1 1000 ps trajectory onto the two first principal components. The folded conformation corresponds to negative values of PC1.

aptitude of GLP-1 allows an environment-dependent conformational switch: it is a known fact that some amphiphilic peptides can form helical structures when in an hydrophobic environment [34,35]. Thornton noted that the distortion between the two helical segments can align their hydrophobic faces on a single side of the peptide and favor hydrophobic interaction with the membrane. Amide exchange data suggest that the hydrophobic portions of the helices are buried in the micelle. The MLP calculation shows two distinct hydrophilic/hydrophobic sides in the peptide in Thornton conformation, allowing interactions with the hydrophobic phase in a carpet-like style or the dimerization of peptides. Nevertheless, the folded conformation in water is characterized by the loss of the amphiphilic property of the peptide (Figure 4). The peptide moves toward a distinct medium-dependent conformation: the two hydrophobic clusters formed in lipidic environment move face-to-face to form a buried hydrophobic core, breaking the spatial clustering of

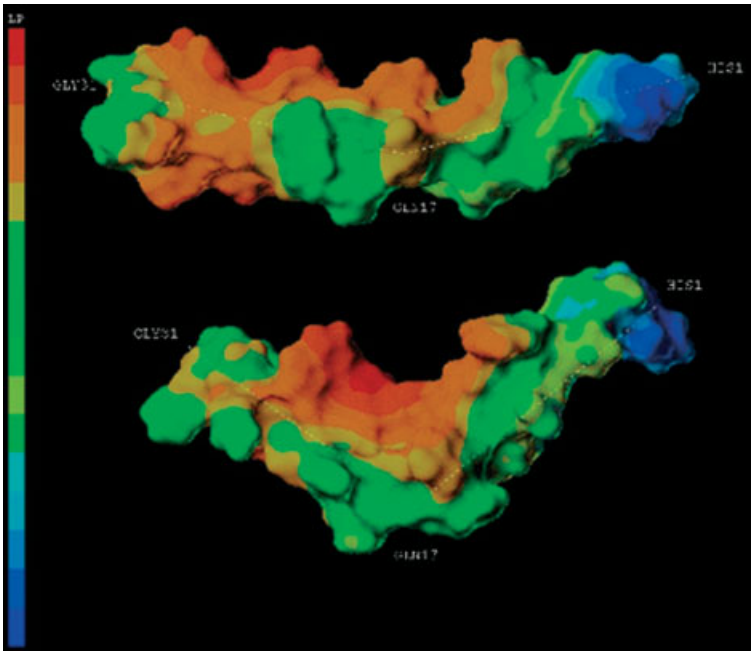

Figure 4 Hydrophilic (blue) and hydrophobic (red) molecular potential of GLP-1 in the Thornton conformation (top) and in the folded conformation after 1000 ps MD trajectory (bottom).

hydrophobic regions over one side that characterizes interactions with biological membranes. Such a folded conformation has not been observed *in vitro* and its potential role remains unknown, but its implication as a folded bound bioactive conformation has been questionned. In particular, we wanted to check whether this characteristic dynamic feature of GLP-1 holds for all active analogs in a similar time scale, as a marker for determining internal constraints or internal interactions in the simulated structure.

GLP-1 Analog Molecular Dynamics

The question arose if a turn or a fold is required for full biological activity. In such a case, peptide folding should be considered as a necessary but insufficient condition for full biological activity. Indeed, an active analog should exhibit a folding as well as local requirements compatible with receptor interactions. On the contrary, the absence of any folding could strongly indicate a lack of activity. It was necessary to check if the very characteristic dynamics profile of GLP-1 can be considered as a marker of activity and to evaluate how the active analogs of GLP-1 could reproduce it in the same conditions of simulation. Among the three GLP-1 analogs modified at position 1, only [F1]-GLP-1 exhibits both high activity and affinity, whereas [Y1]-GLP-1 and [W1]-GLP-1 have medium affinity. However, none of these GLP-1 analogs modified at position 1 exhibit a dynamic behavior similar to that of GLP-1 itself (Figures 5 and 6). The weak antagonist [W1]-GLP-1 folds up to a bend angle of about 110° but the dynamic fingerprints clearly show that it does not reach the point of transition to the folded conformation area. It was established that mutations at position 1 strongly influence MD trajectories with respect to GLP-1 but the absence of any early folding can in no way be predictive of a lack of affinity or activity. In the same way, it was observed that mutations at position 2 allow the two inactive peptides [L2]-GLP-1 and [S2]-GLP-1 to explore a wider conformational space than the two active peptides [V2]-GLP-1 and [a2]-GLP-1. Although the two active analogs exhibit a rather similar dynamics profile, they remain more distant from the GLP-1 trajectory than inactive analogs. In any case, mutations at position 2 prevent a clear folding of the peptide (Figures 7 and 8). The presence of His1 and Ala2 seems to be crucial for GLP-1 folding and the characteristic dynamics profile but not for full biological activity.

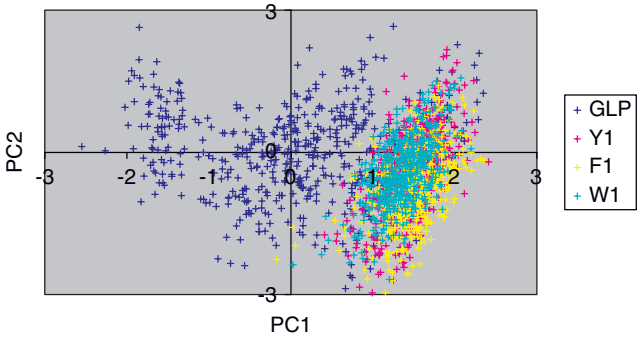

Figure 5 Projection of trajectories for GLP-1 analogs mutated at position 1 onto the principal components PC1 and PC2. No trajectories explore the folded conformation area of the GLP-1 trajectory.

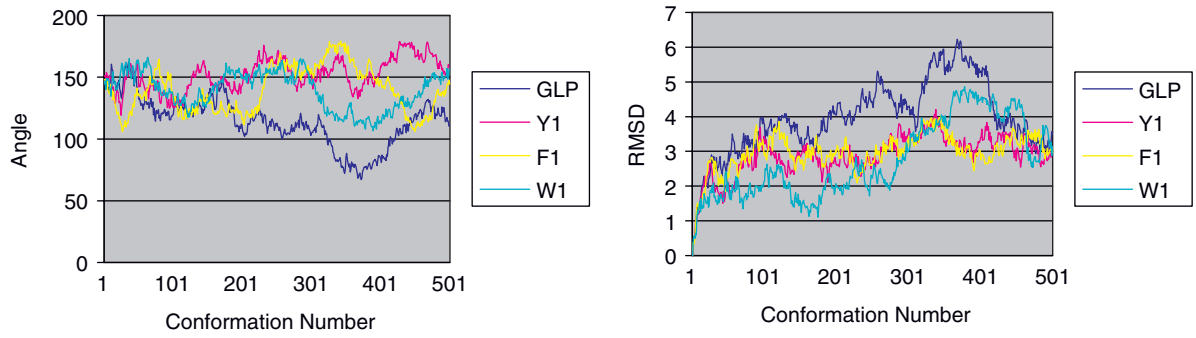

Figure 6 Monitoring of bend angle (Cα[1]-Cα[17]-Cα[31]) and RMS Deviation of GLP-1 analogs modified at position 1 during a 1000 ps MD trajectory (1 conformation saved every 1 ps).

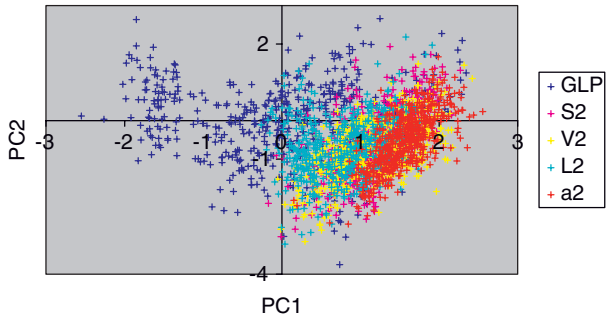

Figure 7 Projection of trajectories for GLP-1 analogs mutated at position 2 onto the principal components PC1 and PC2. No trajectories explore the folded conformation area of the GLP-1 trajectory.

These results confirm the strong influence of positions 1 and 2 on the global dynamics of GLP-1 analogs in our simulation conditions but an absence of correlation between the estimated flexibility of the peptide and its biological activity or affinity. However, it may be that these observations are due to the fact that the folded conformations exhibit some unfavorable local physico-chemical features that disadvantage peptide–receptor interactions.

CONCLUSION

Whilst it is acknowledged that short simulations may be insufficient for establishing dynamic–activity relationships, even in some rather standard conditions of calculation, nonetheless the dynamic fingerprint can be considered as a conformational descriptor measuring the level of 'dynamic behaviour' similarity for two different molecules. The automatization of a standardized procedure of 3D ACM provides access to such information from the molecular dynamics trajectories data easily and quickly and constitutes a powerful tool for investigating the relatively unexplored field of dynamic–activity relationships. This has already been successfully used for dynamic–activity relationships of immunosuppressive peptides in our laboratory [18]. In this study, the role of the conformational flexibility of the central part of GLP-1(7–36)amide was investigated using molecular dynamics and a 3D autocorrelation method. Our goal was to apply the 3D ACM and to check if peptide folding can be used as a marker or 'fingerprint' for activity or affinity. For this purpose, we had (i) to apply the 3D ACM to a set of peptide analogs, (ii) to prospect the conformational landscape of GLP-1 and its analogs and (iii) to determine whether the dynamic fingerprint of a peptide can discriminate between different analogs by limiting some conformational area compatible with the activity. The GLP-1 has been chosen for its hypothesized, but not yet proven,

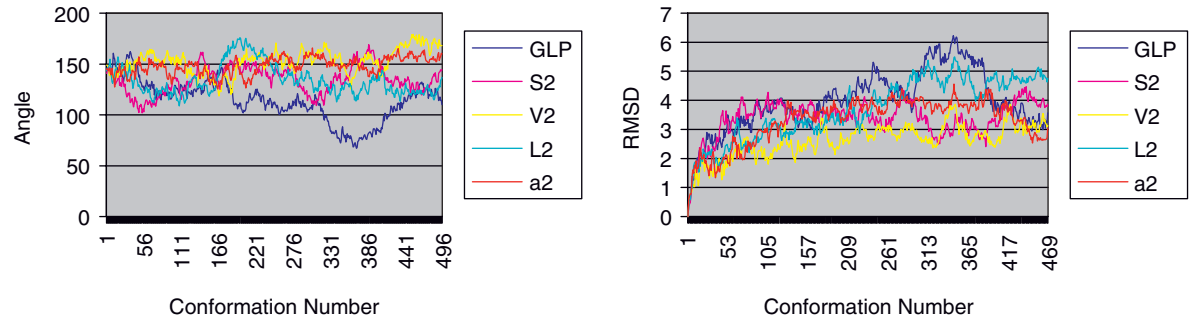

Figure 8 Monitoring of bend angle (Cα[1]-Cα[17]-Cα[31]) and RMS Deviation of GLP-1 analogs modified at position 2 during a 1000 ps MD trajectory (1 conformation saved every 1 ps).

tendency to fold towards a more compact conformation and the uncertainties about its bioactive conformation. Furthermore, GLP-1 is actually a good drug candidate for the treatment of non-insulin-dependent diabetes mellitus and obesity and this work was accompanied by the design of new drug candidates. In accordance with some experimental results, the GLP-1 molecular dynamics simulation suggests that the conformation can switch to a more compact conformation when in an aqueous environment, this is accompanied by a loss of its amphiphilic feature. The examination of the trajectories for seven GLP-1 analogs, varied at key positions 1 and 2, has shown that the folding of GLP-1 in an aqueous environment does not explain the difference between the active and inactive GLP-1 analogs. Consequently, these results do not support the hypothesis of a folded-bioactive conformation of GLP-1.

Acknowledgement

We would like to thank Les Laboratoires Servier for their financial support.

REFERENCES

1. Thorens B. Expression cloning of the pancreatic beta cell receptor for the gluco-incretin hormone glucagon-like peptide 1. *Proc. Natl Acad. Sci. USA* 1992; **89**: 8641–8645.
2. Kawai K, Ohse C, Watanabe Y, Suzuki S, Yamashita K, Ohashi S. Pituitary adenylate cyclase activating polypeptide stimulates insulin release from the isolated perfused rat pancreas. *Life Sci.* 1992; **50**: 257–261.
3. Mojsov S. Structural requirements for biological activity of glucagon-like peptide-I. *Int. J. Pept. Protein Res.* 1992; **40**: 333–343.
4. Adelhorst K, Hedegaard BB, Knudsen LB, Kirk O. Structure-activity studies of glucagon-like peptide 1. *J. Biol. Chem.* 1994; **269**: 6275–6278.
5. Gallwitz B, Witt M, Paetzold G, Morys-Wortmann C, Zimmermann B, Eckhart K, Fölsch UR, Schmidt WE. Structure/activity characterization of glucagon-like peptide-1. *Eur. J. Biochem.* 1994; **225**: 1151–1156.
6. Thornton K, Gorenstein DG. Structure of glucagon-like peptide (7–36) amide in a dodecylphosphocholine micelle as determined by 2D NMR. *Biochemistry* 1994; **33**: 3532–3539.
7. Montrose-Rafizadeh C, Eng J. Agonist secondary structure correlates with binding affinity to GLP-1 receptor. In *57th Annual Meeting & Scientific Sessions, Hynes Convention Center, Boston, 1997, June 21–24*, poster N°725.
8. Braun W, Wider G, Lee KH, Wüthrich KJ. Conformation of glucagon in a lipid-water interphase by 1H-NMR. *Mol. Biol.* 1983; **169**: 921–948.
9. Parker JC, Andrews KM, Rescek DM, Massefski Jr W, Andrews GC, Contillo LG, Stevenson RW, Singleton DH, Suleske RT. Structure-function analysis of a series of glucagons-like peptide-1 analogs. *J. Peptide Res.* 1998; **52**: 398–409.
10. Goke R, Fehmann HC, Linn T, Schmidt H, Krause M, Eng J, Goke B. Exendin-4 is a high potency agonist and truncated exendin-(9–39)-amide an antagonist at the glucagon-like peptide 1-(7–36)-amide receptor of insulin-secreting beta-cells. *J. Biol. Chem.* 1993; **268**: 19 650–19 655.
11. Yasri A, Chiche L, Haiech J, Grassy G. Rational choice of molecular dynamics simulation parameters through the use of the three-dimensional autocorrelation method: application to calmodulin flexibility study. *Protein Eng.* 1996; **9**: 959–976.
12. Gros L, Thorens B, Bataille D, Kervran A. Glucagon-like peptide-1-(7–36) amide, oxyntomodulin, and glucagon interact with a common receptor in a somatostatin-secreting cell line. *Endocrinology* 1993; **326**: 1316–1322.
13. Bradford MM. A rapid and sensitive method for the quantitation of microgram quantities of protein utilizing the principle of protein-dye binding. *Anal. Biochem.* 1976; **72**: 248–254.
14. Steiner AL, Parker CW, Kipnis DM. Radioimmunoassay for cyclic nucleotides. I. Preparation of antibodies and iodinated cyclic nucleotides. *J. Biol. Chem.* 1972; **247**: 1106–1113.
15. Steiner AL, Pagliara AS, Chase LR, Kipnis DM. Radioimmunoassay for cyclic nucleotides. II. Adenosine 3′,5′-monophosphate and guanosine 3′,5′-monophosphate in mammalian tissues and body fluids. *J. Biol. Chem.* 1972; **247**: 1114–1120.
16. Steiner AL, Wehmann RE, Parker CW, Kipnis DM. Radioimmunoassay for the measurement of cyclic nucleotides. *Adv. Cyclic. Nucleot. Res.* 1972; **2**: 51–61.
17. URL: http://www.accelrys.com
18. Grassy G, Calas B, Yasri A, Lahana R, Woo J, Iyer S, Kaczorek M, Floc'h R, Buelow R. Computer-asssisted rational design of immunosuppressive compounds. *Nature Biotechnol.* 1998; **16**: 748–752.
19. Broto P, Moreau G, Vandycke C. Molecular structures: perception, autocorrelation descriptor and SAR studies. Autocorrelation descriptors. *Eur. J. Med. Chem.* 1984; **19**: 66–70.
20. Fauchère JL, Quarendon P, Kaetterer L. Estimating and representing hydrophobicity potential. *J. Mol. Graphics* 1988; **6**: 203–206.
21. Ghose AK, Crippen GM. Atomic physicochemical parameters for three-dimensional-structure-directed quantitative structure-activity relationships. 2. Modeling dispersive and hydrophobic interactions. *J. Chem. Inf. Comput. Sci.* 1987; **1**: 21–35.
22. Mentlein R, Gallwitz B, Schmidt WE. Dipeptidyl-peptidase IV hydrolyses gastric inhibitory polypeptide, glucagon-like peptide-1(7–36)amide, peptide histidine methionine and is responsible for their degradation in human serum. *Eur. J. Biochem.* 1993; **214**: 829–835.
23. Deacon CF, Johnsen AH, Holst JJ. Degradation of glucagon-like peptide-1 by human plasma in vitro yields an *N*-terminally truncated peptide that is a major endogenous metabolite *in vivo*. *J. Clin. Endocrinol. Metab.* 1995; **80**: 952–957.
24. Deacon CF, Knudsen LB, Madsen K, Wiberg FC, Jacobsen O, Holst JJ. Dipeptidyl peptidase IV resistant analogues of glucagon-like peptide-1 which have extended metabolic stability and improved biological activity. *Diabetologia* 1998; **41**: 271–278.
25. Kieffer TJ, McIntosh CH, Pederson RA. Degradation of glucose-dependent insulinotropic polypeptide and truncated glucagon-like peptide 1 *in vitro* and *in vivo* by dipeptidyl peptidase IV. *Endocrinology* 1995; **136**: 3585–3596.
26. Pauly RP, Rosche F, Wermann M, McIntosh CH, Pederson RA, Demuth HU. Investigation of glucose-dependent insulinotropic polypeptide-(1–42) and glucagon-like peptide-1-(7–36) degradation *in vitro* by dipeptidyl peptidase IV using matrix-assisted laser desorption/ionization-time of flight mass spectrometry. A novel kinetic approach. *J. Biol. Chem.* 1996; **271**: 23 222–23 229.
27. Goke R, Hareter A, Vahl T, Bode HP, Hoffmann E. The insulinotropic gut hormone glucagon-like peptide-1. In *Front Diabetes*, Fehmann HC, Goke B (eds). Karger: Basel, 1997; 13, 85–104.
28. Burcelin R, Dolci W, Thorens B. Long-lasting antidiabetic effect of a dipeptidyl peptidase IV-resistant analog of glucagon-like peptide-1. *Metabolism* 1999; **48**: 252–258.
29. Unson CG, Macdonald D, Ray K, Durrah TL, Merrifield RB. Position 9 replacement analogs of glucagon uncouple biological

activity and receptor binding. *J. Biol. Chem.* 1991; **266**: 2763–2766.
30. Unson CG, Macdonald D, Merrifield RB. The role of histidine-1 in glucagon action. *Arch. Biochem. Biophys.* 1993; **300**: 747–750.
31. Unson CG, Wu CR, Merrifield RB. Roles of aspartic acid 15 and 21 in glucagon action: receptor anchor and surrogates for aspartic acid 9. *Biochemistry* 1994; **33**: 6884–6887.
32. Unson CG, Wu CR, Fitzpatrick KJ, Merrifield RB. Multiple-site replacement analogs of glucagon. A molecular basis for antagonist design. *J. Biol. Chem.* 1994; **269**: 12 548–12 551.
33. Unson CG, Merrifield RB. Identification of an essential serine residue in glucagon: implication for an active site triad. *Proc. Natl Acad. Sci. USA* 1994; **91**: 454–458.
34. Bruch MD, Hoyt DW. Conformational analysis of a mitochondrial presequence derived from the f1-ATPase beta subunit by CD and NMR spectroscopy. *Biochem. Biophys. Acta* 1992; **1159**: 81–93.
35. Karslake C, Piotto ME, Pak YM, Weiner H, Gorenstein DG. 2D-NMR and structural model for a mitochondrial signal peptide bound to a micelle. *Biochemistry* 1990; **29**: 9872–9878.
36. Adenot M, Sarrauste de Menthière C, Chavanieu A, Calas B, Grassy G. Peptide quantitative structure-activity relationships: an automated mutation strategy to design peptides and pseudo-peptides from substitution matrices. *J. Mol. Graph. Model.* 1999; **17**: 292–309.
37. Hareter A, Hoffmann E, Bode HP, Goke B, Goke R. The positive charge of the imidazole side chain of histidine 7 is crucial for the GLP-1 action. *Endocr. J. (Tokyo)* 1997; **44**: 701–705.